Maximum Power Point Tracking Using Modified Butterfly Optimization Algorithm for Partial Shading, Uniform Shading, and Fast Varying Load Conditions

Immad Shams, *Student Member, IEEE*, Saad Mekhilef, *Senior Member, IEEE*, and Kok Soon Tey, *Member, IEEE*

***Abstract*—In this article, a new maximum power point tracking algorithm based on a modified butterfly optimization algorithm has been proposed. The proposed method is capable of differentiating between different partial shading patterns, uniform shading, solar intensity, and load variation conditions with fast convergence speed (CS). Only one dynamic variable is used as a tuning parameter reducing the complexity of the algorithm. The search space skipping method has been proposed to improve the CS. The proposed method is hybridized with a constant impedance method to improve the response time of the system for fast varying load variations. The proposed method has been validated experimentally on the SEPIC converter topology with a sampling time of 0.05 s. The experimental validation proved the average tracking time for different shading patterns is less than 1 s with steady-state efficiency of 99.85% on average. The CS for uniform shading conditions is improved by 47.20%. The response to load variation is also improved by 86.15% and becomes eligible to be utilized for fast varying load variations. Finally, the comparison table based on the MPPT rating has been presented to determine the effectiveness of the proposed method among other popular metaheuristic approaches used for MPPT.**

***Index Terms*—Butterfly optimization algorithm, global maximum power point, maximum power point tracking (MPPT), metaheuristic algorithms.**

NOMENCLATURES

c	Sensory modality.
$D_i(t)$	Duty cycle of the *i*th particle in the current iteration.
$D_{Gbest}(t)$.	Global best duty cycle in the search space.
D_{MPP}	Duty cycle at MPP.
$D_{besti}(t)$	Best duty cycle of the *i*th particle.
$D_s(t)$	Sampled duty cycle.
$f(t)$	Fragrance.
$I(t)$	Stimulus intensity.
I_{MPP}	Current at MPP.
$I_{\rm PV}$	PV current.
I_{sc}	Short-circuit current.
P	Probability condition.
$P_{Gbest}(t)$	Global best power.
P_{MPP}	Power at MPP.
P_{PV}	PV power.
P_{besti}	Best power of the *i*th particle.
$P_i(t)$	Power of the *i*th particle.
r	Random number.
t	Number of iteration.
$t_{\max}$	Maximum number of iterations.
V_{MPP}	Voltage at MPP.
V_{PV}	PV voltage.
V_{oc}	Open-circuit voltage.
$x_{best}(t)$	Best position of a particle.
$x_i(t), x_j(t), x_k(t)$	Position of *i, j,* and *k* particles in the search space.
$Z_{\rm in}$	Input impedance.
Z_{MPP}	Impedance at MPP.
$Z_{\rm out}$	Output impedance.
a	Power exponent.
ΔD	Difference of duty cycle between each particle.
φd	Fixed perturbation of duty cycle.

Manuscript received June 12, 2020; revised September 1, 2020; accepted October 3, 2020. Date of publication October 8, 2020; date of current version January 22, 2021. This work was supported in part by the University of Malaya Impact Oriented Interdisciplinary Research Grant under Grant IIRG011C-2019 and in part by the NICOP Research under Grant N62909-18-1-2030 (UM Project IF011-2018). Recommended for publication by Associate Editor A. Canesin. (*Corresponding author: Saad Mekhilef.*)

Immad Shams is with the Power Electronics and Renewable Energy Research Laboratory, Department of Electrical Engineering, University of Malaya, Kuala Lumpur 50603, Malaysia (e-mail: immadshams@um.edu.my).

Saad Mekhilef is with the Power Electronics and Renewable Energy Research Laboratory, Department of Electrical Engineering, University of Malaya, Kuala Lumpur 50603, Malaysia, and also with the School of Software and Electrical Engineering, Faculty of Science, Engineering and Technology, Swinburne University of Technology, Victoria, VIC 3122, Australia (e-mail: saad@um.edu.my).

Kok Soon Tey is with the Department of Computer System and Technology, Faculty of Computer Science and Information Technology, University of Malaya, Kuala Lumpur 50603, Malaysia (e-mail: koksoon@um.edu.my).

Color versions of one or more of the figures in this article are available online at https://ieeexplore.ieee.org.

Digital Object Identifier 10.1109/TPEL.2020.3029607

I. INTRODUCTION

THE world energy demand is increasing day by day due to the increase in the population [1], increased lifestyle, and the development of new technologies such as electric vehicles, power electronic devices, state-of–the-art machinery, etc. Each new application requires energy in one form or another. The depletion of primary energy sources such as coal and fossil fuel is also of great concern [2]. These circumstances are the primary cause of attention to renewable energy resources. Solar energy gets special attention due to its sustainability, availability

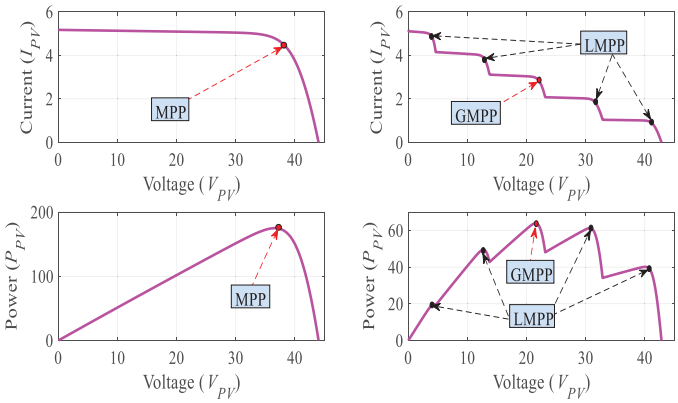

Fig. 1. *P–V* and *I–V* curves.

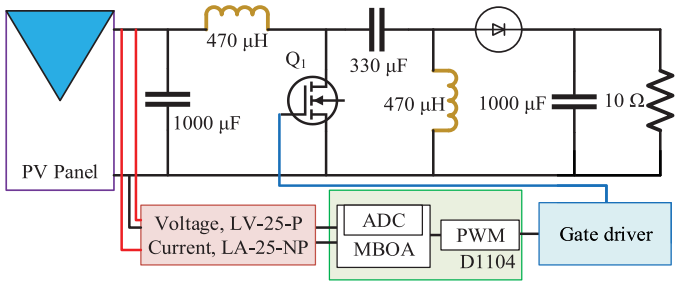

Fig. 2. DC–DC SEPIC topology.

in abundance, pollution free, and carbon emission-free nature. Currently, more than hundred countries are utilizing PV systems for standalone and grid-connected applications. International Energy Agency for Photovoltaic Power Systems (IEA-PVPS) predicted that by the end of 2020, the worldwide installed PV capacity is expected to be expanded up to 500 GW [3], [4].

The solar energy is dependent on the temperature and irradiance conditions [5]. The current–voltage (*I–V*) and power–voltage (*P–V*) curves are nonlinear in nature. Under normal conditions, the *P–V* curve exhibits a unique maximum power point (MPP), as shown in Fig. 1. Hence, it is quite essential to operate the PV array at MPP, which is made possible with the help of maximum power point tracking (MPPT) controller. MPPT is used with the aid of a power electronic converter that is installed between the load and PV source, as shown in Fig. 2. The solar array consists of series-connected solar modules to provide the grid-connected inverters with high voltage input. The series connection requires all modules to generate the same amount of current. The shaded modules are unable to produce the same amount of current as of the unshaded one under partial shading condition (PSC) [6]. Hence, the shaded module will consume instead of supplying current. As a consequence, an avalanche breakdown can occur which can create a hotspot on the panel surface [7]. In order to prevent the hotspot phenomenon, bypass diodes are used in parallel via the modules to simply bypass the shaded modules and this causes the multiple peaks on the *P–V* and *I–V* curves. The multiple peaks consist of multiple local maximum power points (LMPPs) and one global maximum power point (GMPP), as shown in Fig. 1 [8].

MPPT is a hot topic of research hence numerous MPPT algorithms are proposed in the literature. The conventional algorithms like perturb and observe (P&O), hill climbing and incremental conductance (IncC) [16] are straightforward algorithms with fast tracking speed. The problems associated with them are, however, oscillation around MPP, indirect control of the duty cycle requiring the adjustment of PID/PI parameters, modification required to adjust the direction of the duty cycle perturbation with the switch of the converter (i.e., from buck to boost), and their range of tracking is local search space [9], [10], [11], [12]. This is because of their way of approaching the MPP by perturbing the voltage and observing the power. When the operating point is in the LMPP zone, it will keep oscillating around LMPP and will not be able to scan for the GMPP region during mismatch conditions.

The modification to the conventional MPPT algorithms was proposed to rectify the problems associated with conventional controllers against GMPP tracking in [13]–[15]. In general, the standard issue with modified conventional approaches is high convergence time, PV parameters required for implementation within the controller which need to be updated with the passage of time due to degradation of solar cells, modification necessary for the duty cycle update direction with change in the converter, indirect control of the duty cycle, and oscillation around MPP.

The state of the art popular MPPT controllers based on optimization metaheuristic (or bio-inspired) algorithms track the GMPP accurately with high steady-state efficiency [16]–[21]. The biggest benefit of this type of MPPT controller is the direct control of the duty cycle avoiding PID/PI tuning, no requirement of PV parameters for implementation in the controller, simple control structure with less computational burden, no requirement of the duty cycle update path with a shift in the converter and no requirement of a high storage microcontroller makes its implementation simple, cost effective, and robust in comparison with others for complex shading patterns. Despite high-steady-state efficiency, a need for improvement is observed in some areas. Some of the problems associated with metaheuristic algorithms have also been highlighted in [10].

First, repeated exploration of the same position in the search space by the same or other particles was observed using metaheuristic approaches, e.g., in particle swarm optimization (PSO) [16] and differential evolution whale optimization [17]. It will increase the tracking period until the termination criteria are met.

Second, certain coefficients are used as random number generators (r) in metaheuristic approaches, for example, two is multiplied by r in gray wolf optimization (GWO) [20] to decide the value of the *C* parameter. The higher dependence on r for the update of the duty cycle position in a search space may converge the particles toward LMPP as reported in [22].

Third, the bioinspired algorithms have scalability issues, i.e., they need to be tuned as in [21] for differential evolution (DE), mutation factor (*F*), and cross over rate (*CR*). Likewise, the coefficients for fireworks (A, m, a, b, £) require tuning in the fire algorithm [19]. Consequently, the multiple parameters require tuning, which is not made dependent on anything and is given a constant value based on trial and error. It makes these metaheuristic algorithms complex as well.

Fourth, metaheuristic algorithms cannot distinguish between PSCs and uniform shading conditions (USCs) and treat the uniform shaded patterns as partially shaded because same termination condition for PSCs and USCs is used, i.e., artificial bee colony [18] and flower pollination (FP) [23]. Hence, the controller often has to go through several iterations, similar to complex PSCs, to finalize the stabilized duty cycle (D) for USCs, resulting in increased convergence time for USCs.

Fifth, the bioinspired algorithms, such as moth flame optimization [24], monkey king evolution [11], and previously mentioned metaheuristic approaches will reinitialize the particles position for load variation making the system's response to load changes slow.

Sixth, the method of load variations presented in [25] outperforms all the metaheuristic algorithms in terms of convergence speed (CS) to track back the MPP when load variation occurs. However, it depends heavily on the converter used, and the controller will require significant modifications with the shift in converter.

The dc–dc converter selection is also an integral part of the solar MPPT system. However, the in-depth study on the dc-dc converter (buck, boost or buck–boost) for a specific application is out of the scope of this article. SEPIC, as shown in Fig. 2, is used to validate the feasibility of the proposed controller due to its ability to search the entire *P–V* search space [25].

In this article, the modified butterfly optimization algorithm based MPPT controller (MBOA-MPPT) is proposed utilizing one V_{oc} dependent tuning parameter, making the algorithm complexity much simple. Further, the exploration of a position that has already been explored is prevented. During initialization, fixed particle distribution for the implementation of new skipping method is proposed to reduce the search space after the initialization stage, resulted in a fast CS. The differentiating capability between solar intensity and load variation using only one voltage and current sensor is proposed by hybridizing the concept provided in [26] to speed up the response to load variations with the help of newly developed constant impedance approach. Further, the controller does not require major modification with the shift in the converter.

This article proceeds with a discussion on the standard butterfly optimization algorithm. Section III elaborates on the proposed improvement on an MPPT approach. Section IV addressed the improvements proposed for standard BOA considering the proposed improvement in Section III. Section V dealt with various experimental tests and discussions. Section VI compared other popular metaheuristic algorithms to validate the effectiveness of the proposed algorithm based on the MPPT rating. Finally, Section VII concludes the article with future recommendation.

II. Standard Butterfly Optimization Algorithm

In 2019, Arora and Singh proposed the Butterfly Optimization Algorithm (BOA) as a metaheuristic algorithm inspired by butterflies foraging actions as their cooperative step to hunt for food [27]. The smell is the essential sense for butterflies to find the location of food and mating partners even from long distances. Butterflies are used as a population. Each butterfly produces fragrance [$f(t)$], depending on the strength of the stimulus intensity [$I(t)$], the sensory modality (c), and the power exponent (a), as shown in (1). $I(t)$ is related to butterfly fitness. When a butterfly releases higher level of $f(t)$, it will be sensed and intrigued by the other butterflies in the neighboring. $f(t)$ is a key parameter as it will determine how many steps the butterfly will take during the update of the location as shown in (2) and (3)

$$f\,(t) \;=\; c.I(t)^{a}. \tag{1}$$

CS depends heavily on sensory modality (c) in which sensory stands for measure and process the form of energy in a similar way whereas the modality means the sensor's raw input. a is the power exponent to which $I(t)$ is raised. The tuning of c and a allows linear response, regular expression, and response compression. Linear response means that if $I(t)$ increases $f(t)$ also increases in a similar fashion. The regular expression means that if $I(t)$ increases, $f(t)$ increases much higher, whereas the response compression means if $I(t)$ increases, the $f(t)$ will increase much lower.

Once the c parameter is decided for $f(t)$, the next step is to update the butterfly position toward the global best butterfly by (2) or toward local best by (3). Hence, a probability condition (P) is used to switch between local or global search. $x_{best}(t)$ stands for the best position among all butterflies whereas $x_j(t)$ and $x_k(t)$ are the jth and kth butterflies in a search space. The searching process continues until the termination condition is met

$$x_i\,(t) = \begin{cases} x_i(t) + \left(r^2.x_{best}(t) - x_i(t)\right).f(t);\ if\ r\ > P & (2) \\ x_i\,(t) + \left(r^2.x_j\,(t) - x_k\,(t)\right).f\,(t)\,;\ \text{else} & (3) \end{cases}$$

III. Proposed Improvement on an MPPT Approach

In this section, the method to differentiate between USCs and PSCs has been proposed. Then, the skipping method is also proposed to increase the CS for metaheuristic approaches. Furthermore, a new approach for load variations is also proposed to obtain high CS.

A. Search Space Skipping Method During Initialization

With the correct selection of the load parameter, the exploration from V_{oc} to 0 V (at standard test condition) can be achieved by tuning the duty cycle from 0 to 1. When four particles are utilized as a population in a search space with a fixed initial position of $D_1\,(1)$= 0.2, $D_2\,(1)$= 0.4, $D_3\,(1)$= 0.6, and $D_4(1)$ = 0.8 duty cycle, at $D_4(1)$ it will reach to I_{sc} of the PV array. It can be observed from Fig. 3 for shading patterns such as SC-1, SC-2, and SC-3, the PV current at $I_{PV3}(1)$ and $I_{PV4}(1)$ corresponding to $D_3(1)$ and $D_4(1)$ are almost the same because they already reach I_{sc} of the PV array but the voltage difference is high between $D_3(1)$ and $D_4(1)$. Since I_{MPP} is normally at vicinity of $0.9I_{sc}$ of the PV array [28], thus, if the difference between $I_{PV4}(1)$ and $I_{PV3}(1)$ is less than 10%, the condition of (4) can be used to skip the region for searching the GMPP after duty cycle 0.6 till 1.0. Consequently, the search space for four particles position updates will be limited in between 0.2 to 0.6.

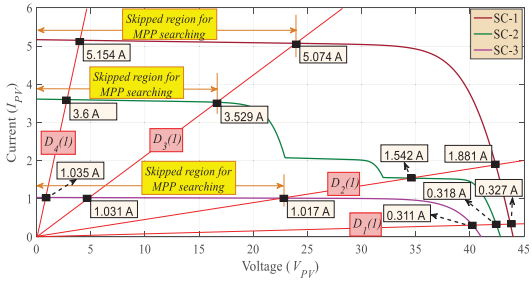

Fig. 3. Determination on skipping region after initialization process.

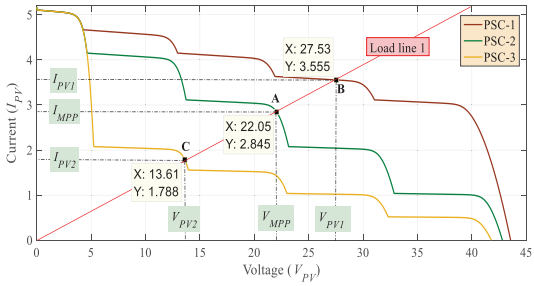

Fig. 4. *I–V* response to dynamic shading variations.

For low irradiance USCs (SC-3), it can be observed that $I_{PVi}(1)$ for $D_4(1)$, $D_3(1)$, and $D_2(1)$ are almost the same since they are in the region of I_{sc} of a PV array. Therefore, the condition of (5) can be used to skip the region after duty cycle 0.4, and the subsequent search space for four particles positions will be updated in between 0.2 to 0.4 duty cycle only. This proposed method will increase the CS for USCs by reducing the search space to determine the MPP.

The same concept can be applied to PSCs (SC-2) who give almost the same $I_{PVi}(1)$ at $D_3(1)$ and $D_4(1)$ during the initialization process and thus, the search space for GMPP tracking will be reduced as well by using (4)

$$\begin{bmatrix} \text{If } I_{PV4}(1) - I_{PV3}(1) < 10\% \\ \text{at } D_4(1) \text{ and } D_3(1) \\ \text{Skip the region of } D \text{ from 0.6 to 1} \end{bmatrix} \tag{4}$$

$$\begin{bmatrix} \text{If } I_{PV4}(1) - I_{PV3}(1) < 10\% \text{ and} \\ \text{If } I_{PV4}(1) - I_{PV2}(1) < 10\% \\ \text{at } D_4(1),\ D_3(1),\ D_2(1) \\ \text{Skip the region of } D \text{ from 0.4 } to \text{ 1} \end{bmatrix}. \tag{5}$$

B. Differentiate Between Solar Intensity and Load Variation

Let us suppose for PSC-2 in Fig. 4, the maximum power operating point (P_{MPP}) is at point A, in which the PV current is at I_{MPP} (2.845 A) and PV voltage is at V_{MPP} (22.05 V). When PSC variation occurs from PSC-2 to PSC-1, the operating point will be shifted from point A to B and the voltage (V_{PV1}= 27.53 V) and current (I_{PV1}= 3.555 A) will be increased in comparison with V_{MPP} and I_{MPP} tracked for PSC-2 on load line 1. Similarly, when PSC variation occurs from PSC-2 to PSC-1, the operating point will be shifted from point A to C and the voltage (V_{PV2}= 13.61 V) and current (I_{PV2}= 1.788 A)

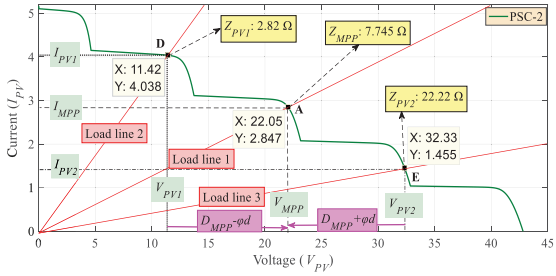

Fig. 5. Proposed method to response for load variations.

will be reduced in comparison with V_{MPP} and I_{MPP} tracked for PSC-2. Hence, it can be said that the solar intensity variation occurred when (6) gets satisfied [26].

For load variation, let us suppose P_{MPP} is at point A in Fig. 5 for load line 1, in which the PV current is at I_{MPP} (2.847 A) and PV voltage is at V_{MPP} (22.05 V). When the load increased from load line 1 to 2, it resulted in the shift of operating point from point A to D. The decrease in voltage (V_{PV1}= 11.42 V) caused an increase in current (I_{PV1}= 4.038 A) in comparison with V_{MPP} and I_{MPP} tracked at point A on load line 1. Similarly, if the load decreased from load line 1 to 3, the operating point will be shifted from point A to E. The voltage (V_{PV2}= 32.33 V) increased but the current (I_{PV2}= 1.455 A) decreased in comparison with V_{MPP} and I_{MPP} tracked at point A for load line 1. Hence, it can be said that the load variation occurred if the condition of (7) gets satisfied [25]. Hence, by using (6) or (7) the distinguishing capability between solar intensity and load variations can be achieved

$$\begin{bmatrix} V_{PV}(t) > V_{MPP} \text{ and } I_{PV}(t) > I_{MPP} \\ \text{OR} \\ V_{PV}(t) < V_{MPP} \text{ and } I_{PV}(t) < I_{MPP} \end{bmatrix} \tag{6}$$

$$\begin{bmatrix} V_{PV}(t) > V_{MPP} \text{ and } I_{PV}(t) < I_{MPP} \\ \text{OR} \\ V_{PV}(t) \langle V_{MPP} \text{ and } I_{PV}(t) \rangle I_{MPP} \end{bmatrix}. \tag{7}$$

C. Constant Impedance Method for Fast Varying Load

When the load variation occurs, Z_{MPP} (V_{MPP}/ I_{MPP}= 7.745 Ω) does not change and only the duty cycle toward Z_{MPP} changes, as shown in Fig. 5. Hence, by keeping Z_{MPP} as a reference and with fixed perturbation of φd toward Z_{MPP}, the GMPP can be tracked back for load variations. The direction of perturbation can be decided by condition (8) and (9). If $Z_{PV}(t)$ (Z_{PV2}= 22.22 Ω in Fig. 5) is greater than Z_{MPP}, means the load is decreased and the load line is moved toward the right side on the *I–V* curve. To brought it back toward Z_{MPP}, the increase in duty cycle is required by condition of (8), as illustrated in Fig. 5, and vice versa if $Z_{PV}(t)$ (Z_{PV1}= 2.82 Ω in Fig. 5) is lower than Z_{MPP} by condition of (9)

$$D_{MPP} = \begin{cases} D_{MPP} + \varphi d;\ If\ Z_{PV}(t) > Z_{MPP} & (8) \\ D_{MPP} - \varphi d;\ If\ Z_{PV}(t) < Z_{MPP} & (9) \end{cases}$$

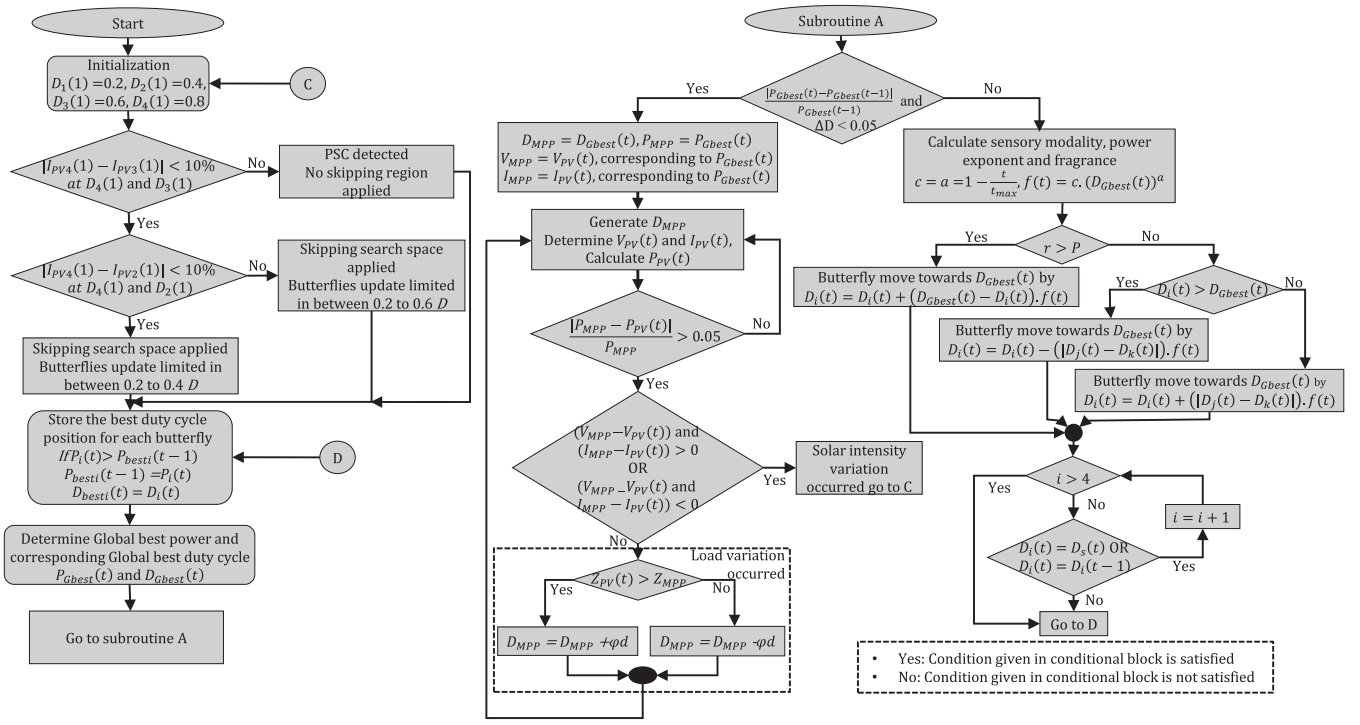

Fig. 6. Flowchart of the proposed algorithm.

The value of φd can be chosen based on trial and error, since a small value may cause a decrease in CS but a high value may cause oscillation around MPP. Therefore, a tradeoff between CS is needed to avoid oscillation around MPP. When the operating point needs to be moved from right to left using traditional dc–dc converters, it requires an increase in the duty cycle, and vice versa for the left to right. Hence, any traditional isolated or nonisolated dc–dc converter can use this load variation technique without any modification in the direction of perturbation. Furthermore, the proposed approaches can be hybridized with any metaheuristic method used for the MPPT to boost its CS for load and USCs.

IV. Modified BOA for MPPT

In this section, changes to the standard BOA have been suggested considering the proposed improvement on the MPPT approach, MPPT efficiency, and tracking time with its structure as in Fig. 6.

A. Initialization of Butterflies

In terms of MPPT, the number of butterflies represents the number of duty cycles and the butterfly position represents the duty cycle position. Since CS and MPPT efficiency are of higher importance for the MPPT controller, it is observed that four butterflies at equal distance with a fixed initial position of 0.2, 0.4, 0.6, and 0.8 are able to track the peak point of complex shading patterns successfully. The higher number of butterflies will make sure the accuracy of GMPP tracking but will decrease the CS. Hence, a tradeoff is required between the MPPT efficiency and tracking time while selecting the number of butterflies.

B. Skipping Search Space for MPP Tracking

During the initialization process, the condition of (4) and (5) will be utilized as mentioned in Section III to skip the part of the search space for tracking the MPP.

C. Storing Each Butterfly Best Position in a Search Space

The power of each butterfly position is determined and its personal best position $[D_{besti}(t)]$ in a search space will be stored during the tracking state by using the condition of

$$\begin{bmatrix} If\ P_i\,(t) > P_{besti}\,(t-1) \\ P_{besti}\,(t)\ = P_i\ (t) \\ D_{besti}\ (t) = D_i\ (t) \end{bmatrix}. \tag{10}$$

D. Determination of Global Best Position in a Search Space

The global best power $[P_{Gbest}(t)]$ will be selected which is the best power among the personal best power of each butterfly. The butterfly position corresponding to $P_{Gbest}(t)$ will be regarded as $D_{Gbest}(t)$.

E. Termination Condition

Afterward, (11) is used as a termination condition to avoid continuous exploration when two conditions are achieved together. The searching process will terminate when the global best power difference between previous ($P_{Gbest}(t-1)$) and present cycle ($P_{Gbest}(t)$) and the D difference between each butterfly position is less than 5%. This circumstance relates to the four

butterflies being close to each other to make sure the accuracy toward the GMPP has been achieved

$$\frac{|P_{Gbest}(t) - P_{Gbest}(t-1)|}{P_{Gbest}(t-1)} \text{and } \Delta D < 0.05. \tag{11}$$

F. Update of Butterfly's Position

If the condition (11) does not satisfied, the position of each butterfly will be updated with the help of a MBOA-MPPT. In standard BOA, the constant value is assigned to c and a in (1) based on trial and error. In MBOA, c and a are proposed as a dynamic variable and made dependent on the number of iterations (t) as in (12). With the increase in the number of iterations, c and a will become smaller. Thus, the convergence toward peak point become dynamic and accuracy toward GMPP improved. Then, the value of $t_{\max}$ is dependent on V_{oc} of a PV panel. The higher the V_{oc}, the higher the $t_{\max}$. In this article, $t_{\max}$ is chosen as 20. The stimulus intensity $[I(t)]$ is replaced with $D_{Gbest}(t)$ for MPPT, which is corresponding to the global best power in a search space for the update of $f(t)$.

Once $f(t)$ is calculated by (13), the position of each butterfly will be updated by (14) or (15) depending on the probability condition ($P = 0.5$) as shown in Fig. 6. In comparison with (2) and (3), r^2 multiplication with $D_{Gbest}(t)$ in (13) and with $D_j(t)$ in (14) has been avoided. The multiplication of r^2 can cause the premature convergence toward GMPP and the D positioning of butterflies is not getting close to each other, which causes the termination condition of (11) not being satisfied. The only way to stop further exploration and stabilize D is by using the termination condition as a maximum number of iterations. However, the drawback of using a maximum number of iterations as a termination condition is that for any shaded condition it will take the same amount of

$$c(t) = a(t) = \left(1 - \frac{t}{t_{\max}}\right) \tag{12}$$

$$f(t) = \left(1 - \frac{t}{t_{\max}}\right).(D_{Gbest}(t))^{\left(1-\frac{t}{t_{\max}}\right)} \tag{13}$$

$$D_i(t) = D_i(t) + (D_{Gbest}(t) - D_i(t)).f(t) \tag{14}$$

$$\begin{bmatrix} If\ D_i(t) > D_{Gbest}(t) \\ D_i(t) = D_i(t) - (|D_j(t) - D_k(t)|).f(t) \\ If\ D_i(t) < D_{Gbest}(t) \\ D_i(t) = D_i(t) + (|D_j(t) - D_k(t)|).f(t) \end{bmatrix} \tag{15}$$

tracking time to stabilize the duty cycle. Furthermore, the utilization of r^2 will cause an increase in tracking time as well.

According to standard BOA, if the probability condition gets satisfied either the butterfly position will be updated toward the best position by (2) or it will move randomly in a search space by (3). In MBOA-MPPT, (3) has been modified to (15). As a result, the random movement has been directed toward the best position ($D_{Gbest}(t)$) in a searching process, which will cause an improvement in the CS and mature convergence toward the peak point. $D_j(t)$ and $D_k(t)$ will be selected between the other butterflies' position in a search space (j and $k \neq i$).

G. Avoiding the Repeat Exploration of Same Butterfly Position

Equation (14) in MBOA-MPPT may cause the exploration of same position repeatedly, which will increase the tracking time. In order to avoid this issue, the condition of (16) has been utilized to ensure each butterfly compares its position with all the butterfly positions in the previous iteration and with the butterfly's position in the current iteration which has already been sampled to the output. If the condition of (16) gets satisfied, the updated butterfly position will not be sampled to the dc–dc converter to determine the power. Afterward, the next butterfly position will be checked for the same purpose. This condition will improve the CS and the updated butterfly's position which unsatisfied the condition of (16) will be sampled and the process will continue from Section IV-C until the termination criteria of (11) is met

$$\begin{bmatrix} D_i(t) = D_s(t), \text{ where } D_s = \text{ sampled duty } |rmcycle \\ \text{OR} \\ D_i(t) = D_i(t-1) \end{bmatrix}. \tag{16}$$

H. Determining the Solar Intensity or Load Variation

Once the termination condition of (11) is met, $D_{Gbest}(t)$, $P_{Gbest}(t)$, $V_{PV}(t)$, and $I_{PV}(t)$ corresponding to $P_{Gbest}(t)$ will be regarded as D_{MPP}, P_{MPP}, V_{MPP}, and I_{MPP}. The MBOA-MPPT will not be terminated entirely, contrary to the standard BOA, it will move to the next loop to monitor the input power (P_{PV}) at each sample and compare with the stored P_{MPP} as in (17)

$$\frac{|P_{MPP} - P_{PV}(t)|}{P_{MPP}} > 0.05. \tag{17}$$

If the condition (17) is not satisfied, the algorithm will keep generating $D_{MPP,}$ which is corresponding to the best butterfly position. If (17) is satisfied, it means the change in power occurred and it can be due to load or solar intensity variation. The distinction between the two variations is possible by using (6). If (6) gets satisfied means the solar intensity variation occurred else there is a load variation. The MPP tracking will start again from the initialization Section IV-A for solar intensity variation, as in Fig. 6, until the new MPP is tracked.

I. Constant Impedance Method for Load Variation

If the load variation has occurred, the controller will trigger constant impedance method by utilizing the conditions of (8) and (9) as discussed. The constant impedance method perturbs the duty cycle toward Z_{MPP} until P_{MPP} is achieved back as shown in Fig. 6. In this article, φd is taken as 0.04. Hence, the response toward load variation will be much faster in comparison with the reinitialization of butterflies when load variation occurs.

V. Results and Discussions

The SEPIC topology with a sampling time of 0.05 s is chosen to match Z_{in} and Z_{out} for MPPT using the proposed MBOA-MPPT. The PV panel parameters are demonstrated in Table I, whereas the components parameter selected for topology

TABLE I
RATING OF A10J-S72-175 PV MODULE AT STANDARD TEST CONDITIONS (STC) TEMPERATURE = 25 °C AND INSOLATION = 1000 W/m^2

Maximum power (P_{MPP})	175 W
Voltage at MPP (V_{MPP})	36.6 V
Current at MPP (I_{MPP})	4.78 A
Open circuit voltage (V_{OC})	44 V
Short circuit current (I_{SC})	5.17 A

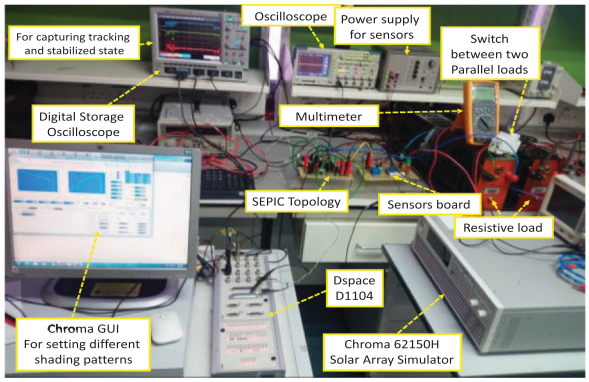

Fig. 7. Experimental setup.

is illustrated in Fig. 2. The PV array is represented with the CHROMA-62150H solar array simulator (SAS) for analysis purposes. The SAS provided with GUI will help us to determine the tracking point in a *P–V* search space effectively. The GUI provided with SAS will be used to test, generate different partial shading patterns, and determine the steady-state MPPT efficiency which is calculated from (18). DSpace (D1104) is used as the central controller to implement the proposed algorithm. Since voltage and current inputs are required for the proposed algorithm, the voltage (LV-25P) and current sensor (LA-25NP) from LEM will sense the voltage and current for DSpace ADC pin. A resistive load of 10 Ω is used. The Lecroy Waverunner 44xi digital storage oscilloscope (DSO) is used to capture the event of tracking and stabilized state. The complete experimental prototype is shown in Fig. 7

$$\text{Steady state MPPT efficiency} = \frac{\text{Stabilized power}}{\text{Maximum available power}} \times 100. \quad (18)$$

A. Different Partial Shading Patterns Validation

Five complex PSCs consisting of five multiple peaks were tested to validate the proposed method. The waveforms of P_{PV}, V_{PV}, I_{PV}, and D during tracking and stabilized state are shown in Fig. 8. The red dot represents the stabilized point on *P–V* and *I–V* search space.

In PSC-A, the shading pattern of five PV modules is set to 1000, 900, 800, 700, and 600 W/m^2 at a constant temperature of 25 °C with maximum available power of 124.1 W. The GMPP location is at the extreme right of P-V search space, as shown in Fig. 8(a). The GMPP tracked with a steady-state efficiency of 99.92% in 0.75649 s. The D calmed at 0.50206.

In PSC-B, the GMPP is in the middle of the four LMPPs as illustrated in Fig. 8(b). GMPP is tracked with 99.89% of steady-state efficiency. The irradiances for five modules are set at 1000, 800, 600, 400, and 200 W/m^2 with maximum available power of 72.26 W. The GMPP was successfully tracked in approximately 0.70698 s. The D steadied at 0.55698.

The GMPP is in the middle of the fourth and third LMPP in PSC-C, as shown in Fig. 8(c). 1000, 800, 700, 600, and 300 W/m^2 are the irradiances set for five PV modules in this condition with maximum available power of 95.57 W. The GMPP successfully tracked with 99.80% of steady-state efficiency in 0.90249 s and the D stabilized at 0.52249.

For PSC-D, as shown in Fig. 8(d), the irradiance values are set at 1000, 600, 250, 150, and 100 W/m^2 with maximum available power of 47.29 W. The GMPP tracked in 0.90378 s with the termination condition for D obtained at 0.63378.

The GMPP on the extreme left of P-V search space regarded as PSC-E, with irradiance values set at 1000, 300, 200, 150, 100 W/m^2 with maximum available power of 35.94 W, has also been validated experimentally, as illustrated in Fig. 8(e). It took 0.51580 s while stabilizing D at 0.76580 with steady-state efficiency of 99.92%.

B. Search Space Skipping Method Validation

To differentiate USCs from PSCs and to highlight the advantage of difference, two tests for the USC has been conducted. First, without skipping the search space for USC and treating the unshaded conditions as the shaded one. Second, with the proposed skipping method. As illustrated in Fig. 9(a), using the traditional procedure, for 1000 W/m^2 on each module named as USC-A, it took about 0.91452 s before the termination condition was met. Whereas, it can be observed that with the aid of search space skipping method during initialization for $D_3(1)$ and $D_4(1)$ for USC in Fig. 9(b), $I_{PV3}(1)$ is approximately equal to $I_{PV4}(1)$. Thus, the duty cycle region from 0.6 was subsequently skipped and the search space is limited in between 0.2 to 0.6 duty cycle in the subsequent tracking which resulted 0.45627 s to satisfy the termination condition. Fig. 9(c) shows that the conventional method tracked the MPP at 0.85976 s (all module with low irradiance of 300 W/m^2, called USC-B), while the proposed method tracked the MPP in 0.60213 s. As can be seen in Fig. 9(d) that during the initialization process $I_{PV2}(1)$, $I_{PV3}(1)$, and $I_{PV4}(1)$ are approximately equal implies that the operating points with duty cycle above 0.4 are near to I_{sc} of the PV array. Hence, the region after 0.4 duty cycle is skipped and the search space is limited in between duty cycle from 0.2 to 0.4. Using this skipping method, the proposed method tracks the USCs quickly with an average CS improvement of 47.20%, as it does not treat the USC as PSC now.

C. Solar Intensity Variation Validation

In standard BOA, once the optimization point is tracked, it cannot be changed online. The MBOA is used to track the GMPP of PSC-A initially as shown in Fig. 10. After the GMPP is tracked at 1.10543 s, the shading pattern is changed to PSC-B and the controller determined that the variation of power

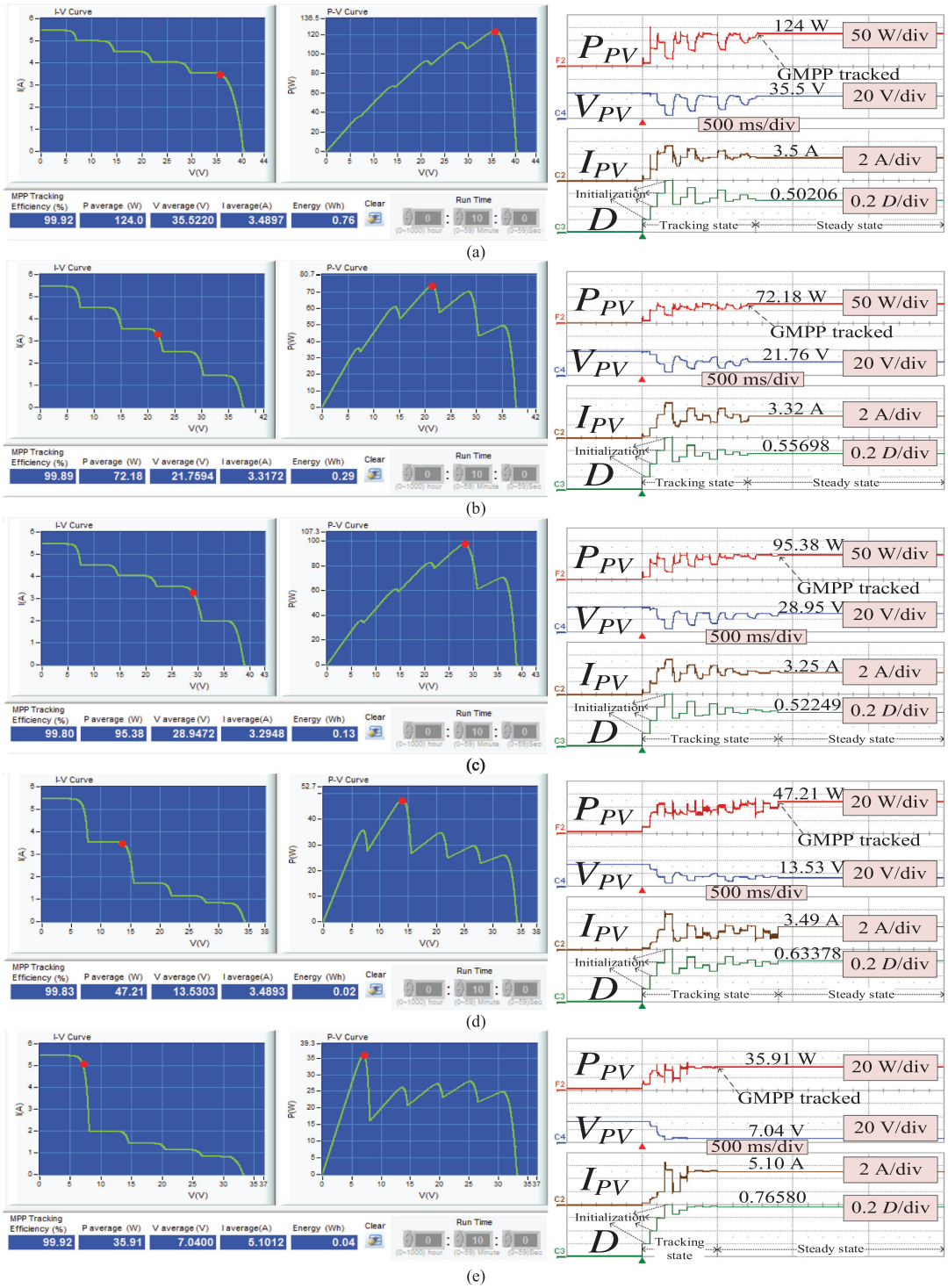

Fig. 8. Experimental validation of the proposed method on (a) PSC-A, (b) PSC-B, (c) PSC-C, (d) PSC-D, and (e) PSC-E.

occurred due to an irradiance change as the voltage and current of PV array decreased. Thus, the reinitialization of tracking process happened and the GMPP for PSC-B was tracked after 0.85385 s. The GMPP was successfully tracked within 0.89428 s after the shading pattern is changed to PSC-D. The proposed method successfully tracked the GMPP for all the PSCs under dynamic shading variations, as shown in Fig. 10.

D. Load Variation Validation

The load variation has been validated experimentally with the help of a switch for abrupt connection and disconnection between two resistive loads connected in parallel, as shown in Fig. 7. To showcase the advantage of the proposed load variation method, two tests are conducted. First, with the conventional

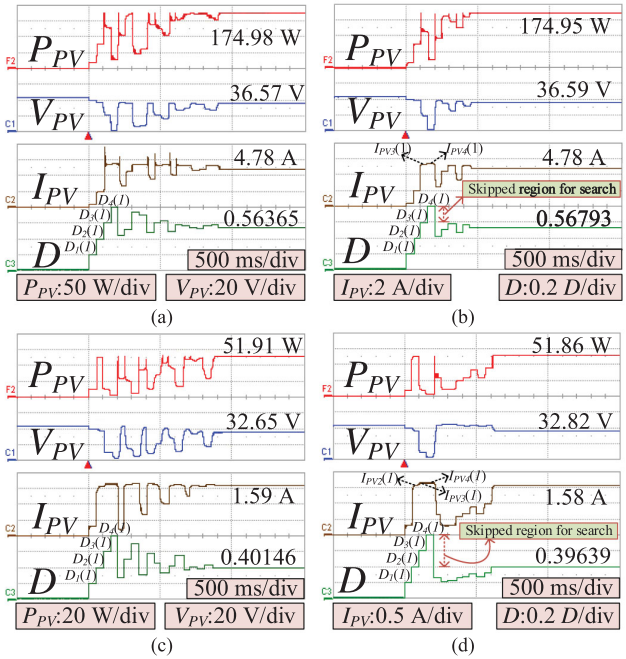

Fig. 9. Experimental comparison for USC-A and B with conventional method (a) and (c) and with search space skipping method (b) and (d).

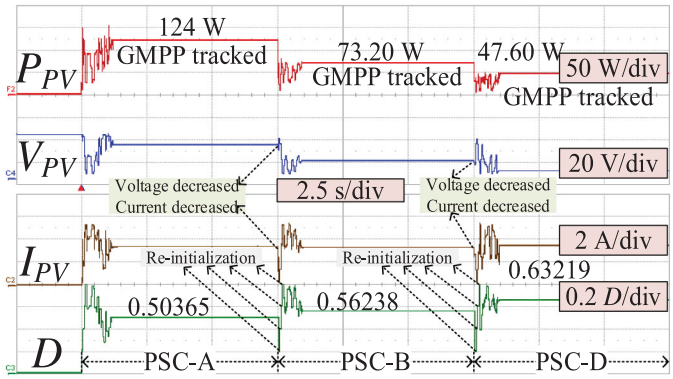

Fig. 10. GMPP variation from PSC-A to PSC-B to PSC-D.

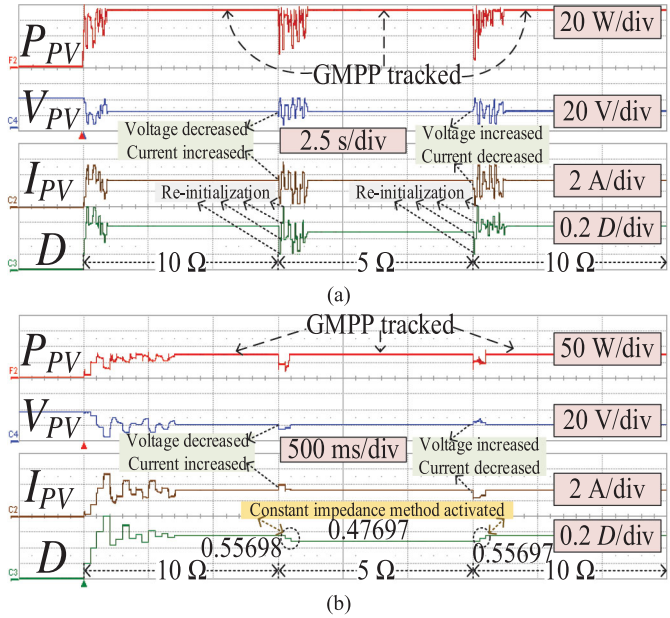

Fig. 11. Load variation test (a) through conventional method (from 10 to 5 Ω) (b) through the proposed method (from 10 to 5 Ω and vice versa).

method of reinitialization of tracking process when load variation occurs, as shown in Fig. 11(a). Second, the proposed constant impedance method for load variation, as shown in Fig. 11(b). The PSC-B was applied with the resistive load of 10 Ω and once the GMPP is tracked, the load was varied from 10 to 5 Ω at 7.5 s in Fig. 11(a) and 1.5 s in Fig. 11(b). It can be observed in Fig. 11(a) that the conventional method with the reinitialization of tracking process requires 1.05163 s to track back the GMPP during the load variation. Then, the load was varied from 5 Ω back to 10 Ω, the reinitialization occurs again, and it took 1.11456 s to track back the GMPP. For our proposed method, as shown in Fig. 11(b), after the GMPP is tracked for PSC-B, the load was varied from 10 to 5 Ω. The controller detected that the change in power occurred due to load variation because the voltage decreased but the current increased. Thus, (9) of the proposed constant impedance method is used to track back the MPP in just 0.15 s. Similarly, when the load was varied from 5 Ω back to 10 Ω, it took 0.15 s to track back the GMPP by bringing back Z_{PV} to Z_{MPP} by using (8). Furthermore, the proposed method avoids the power oscillation in tracking back the GMPP when load variation occurs, as shown in Fig. 11. The proposed method is suitable for fast varying load variations and improves the response to load variation by 86.15% in comparison with traditional technique.

VI. Comparison

The well-established traditional MPPT algorithms such as P&O and Inc., unable to track the GMPP for all PSCs if the tracking point is initially located in the LMPP region. Thus, they are not considered in the comparison section. Therefore, the proposed controller which is the part of bioinspired or metaheuristic MPPT approaches is compared with the state-of-the-art and popular metaheuristic algorithms used for the GMPP tracking to understand the novelty and effectiveness of the proposed method.

The PSC A-E and USC A-B have been utilized to determine the tracking time and steady-state MPPT efficiency for PSO, GWO, FP, and DE using the SEPIC topology with same component parameters and sampling time, as mentioned earlier in the experimental setup, to provide a fair comparison with our proposed method. The PSO has been chosen for comparison because it is treated as a standard for metaheuristic algorithms. The GWO is considered as it utilizes one tuning parameter. FP is included for comparison purpose as it is the state-of-the-art metaheuristic algorithm used for MPPT. Meanwhile, DE has

TABLE II
SELECTION OF TUNING PARAMETERS

MPPT method	Tuning Parameter
PSO	C_{1max}=C_{2max}=2, C_{1min}=C_{2min}=1, w_{max}=1, w_{min}=0.1.
GWO	a=2.
FP	P=0.5, S=0.8, λ=1.5.
DE	F_{min}=0.1, F_{max}=0.4, CR=0.5.

been chosen for comparison in which special attention has been given for load variation.

The value of the tuning parameters of the approaches considering the steady-state efficiency and tracking time, are shown in Table II, on the basis of the trial and error method. The MPPT efficiency has been given superiority when selecting the tuning parameters.

Two types of parameter require the initial setting while using metaheuristic MPPT approaches. First, parameters of tuning are often assigned a constant value based on trial and error. Second, not all the approaches converge toward the best performing position in a search space after each iteration hence they require a maximum number of iterations as termination conditions to stop further exploration and stabilize the duty cycle. The selection of this $t_{\max}$ for the termination condition is also of great importance because it may cause premature convergence if a small value is used. Therefore, these two types of parameters are placed separately in Table III for comparison purposes. Apart from these two parameters, the random number used in the metaheuristic algorithms also affecting the performance of MPPT tracking has been elaborated in Table III.

For fair and accurate comparison through illustration, the simulation results for all the methods are plotted using MATLAB, as in Figs. 12 and 13. GWO outperforms PSO with one tuning parameter for PSCs in terms of CS whereas DE outperformed PSO, GWO, and FP. Since the repeated exploration of the same position is continuously observed for PSO, GWO, FP, and DE in majority of our test cases, which is one of the main reasons that our proposed approach shows fast CS. The example of repeat duty cycle position during tracking state is shown in Fig. 13(a) for the USC-B condition. However, DE demonstrates less repetition of the same positions as compared to PSO, GWO, and FP. This is because it utilized a condition to prevent the exploration of same particle position, which is explored in previous iteration. But another particle in a search space is likely to explore the location of a particle that has been explored. Apart from the repetition of tracking positions, the high ripple in the duty cycle can cause a high voltage stress on the switches which was highlighted in [29]. The FP and GWO show very high duty cycle ripples during the tracking state, but the proposed method avoids the high ripple of duty cycles from one point to another and thus protects the switch from high voltage stress which will increase the lifetime of the control switch as well.

For USCs, as shown in Fig. 13, our proposed method with the help of the skipping method and avoiding the repetition of the same position outperforms all metaheuristic algorithms in terms of CS, as can be observed from average tracking time for USCs in Table III. The proposed method has faster CS in low irradiance USCs due to the high skipping of search space in determining the MPP.

To illustrate a comparison for the transient change in shading patterns, it can be observed from Fig. 14 that the irradiance suddenly decreases from 1000 to 800 W/m^2 and then from 800 to 500 W/m^2 after 3 and 6 s, respectively. The reinitialization of particles occurred when the shading pattern changed abruptly by satisfying the condition of (17). Since the tracking time for MBOA was less in comparison with compared algorithms due to search space skipping method and avoiding the repeat exploration of the explored position, even during irradiance transients, the tracking time of our proposed method is less and will track the new MPP quickly in comparison with other metaheuristic algorithms.

DE outperforms all the described metaheuristic approaches including our proposed method for load variations and reacts very quickly within 100 ms to track back the MPP. However, with the shift in the converter, the DE needs significant modification. Our proposed load variation method reacts faster without any adjustment required in the controller with the shift in the converter and decreases the power oscillation compared to reinitialization during load variations. The other methods will have a slow response to load variations because they will reinitialize the position of particles.

The factors used to determine the MPPT rating through rated mean formula of (19) [10] include number of tuning parameter, number of random numbers, the requirement of $t_{\max}$ for termination, average tracking time considering PSC A-E and USC A-B, MPPT efficiency considering PSC A-E and USC A-B, response to load variations and controller dependence on the system

$$\text{MPPT RATING} = \frac{\text{Total achieved rating}}{7}. \tag{19}$$

1 stand for the best and 4 stands for the worst in Table III. If the specified number of the tuning parameter is one, the rating of 1, two with 2, three with 3, and more than three with 4 shall be given. If the number of random numbers needed is zero, the rating of 1, one with 2, two with 3, and more than two with 4 will be given. Unless the termination condition includes $t_{\max}$, it will be provided with a 2 and if not with 1. When the average tracking time is around 1 s, a rating of 1, between 1 and 2 s with 2, between 2 and 3 s with 3, more than 3 s with 4, will be given. If the efficiency of the MPPT is more than 99%, it will be awarded a rating of 4, between 98% and 99% with 2, between 97% and 98% with 3, less than 97% with 4. If the response to load variations is between 0 and 100 ms, a rating of 1, between 100 ms to 1 s with 2, between 1 to 2 s with 3, more than 2 s with 4 will be issued. If major modification is required in the controller with the change in the converter, this will be granted with 2 and if not with 1.

According to the comparison Table III, the proposed algorithm, with 1.28 rating suggests that it can track the GMPP with fast CS, having the highest number of features in comparison with other metaheuristic techniques used as MPPT. Only one tuning parameter for the MPPT depending on V_{oc} makes its implementation become simpler. The response speed for load

TABLE III
COMPARISON BETWEEN PROPOSED AND OTHER METAHEURISTIC ALGORITHMS

Bio-Inspired MPPT		**PSO [16]**		**GWO [20]**		**FP [17]**		**DE [25]**		**MBOA**	
No. of tuning parameters (rating)		3 (3)		1 (1)		3 (3)		2 (2)		1 (1)	
No. of random numbers (rating)		2 (3)		2 (3)		2 (3)		2 (3)		1 (2)	
t_{max} required as termination condition (rating)		No (1)		Yes (2)		Yes (2)		No (1)		No (1)	
Average tracking time (rating)	PSC-A	1.50 s		1.20 s		2.20 s		1.45 s		0.75 s	
	PSC-B	2.25 s		1.25 s		1.70 s		0.90 s		0.80 s	
	PSC-C	1.95 s		1.25 s		1.60 s		1.35 s		0.60 s	
	PSC-D	1.45 s		2.45 s		1.25 s		0.70 s		0.85 s	
	PSC-E	2.35 s		1.15 s		1.25 s		1.85 s		0.75 s	
	USC-A	1.4 s		1.2 s		2.1 s		1.35 s		0.70 s	
	USC-B	1.35 s		1.95 s		2.45 s		1.15 s		0.60 s	
	Average	PSCs	USCs	PSCs	USCs	PSCs	USCs	PSCs	USCs	PSCs	USCs
		1.90 s	1.375 s	1.46 s	1.575 s	1.6 s	2.275 s	1.25 s	1.25 s	0.75 s	0.65 s
	Overall average	**1.75 s (2)**		**1.49 s (2)**		**1.79 s (2)**		**1.25 s (2)**		**0.72 s (1)**	
Average MPPT efficiency (rating)		99.85% (1)		99.83% (1)		99.82% (1)		99.83% (1)		99.87% (1)	
Response to load variations (rating)		Slow (3)		Slow (3)		Slow (3)		Very fast (1)		Fast (2)	
Controller dependence on system (rating)		No (1)		No (1)		No (1)		Yes (2)		No (1)	
MPPT rating		**2**		**1.86**		**2.14**		**1.71**		**1.28**	

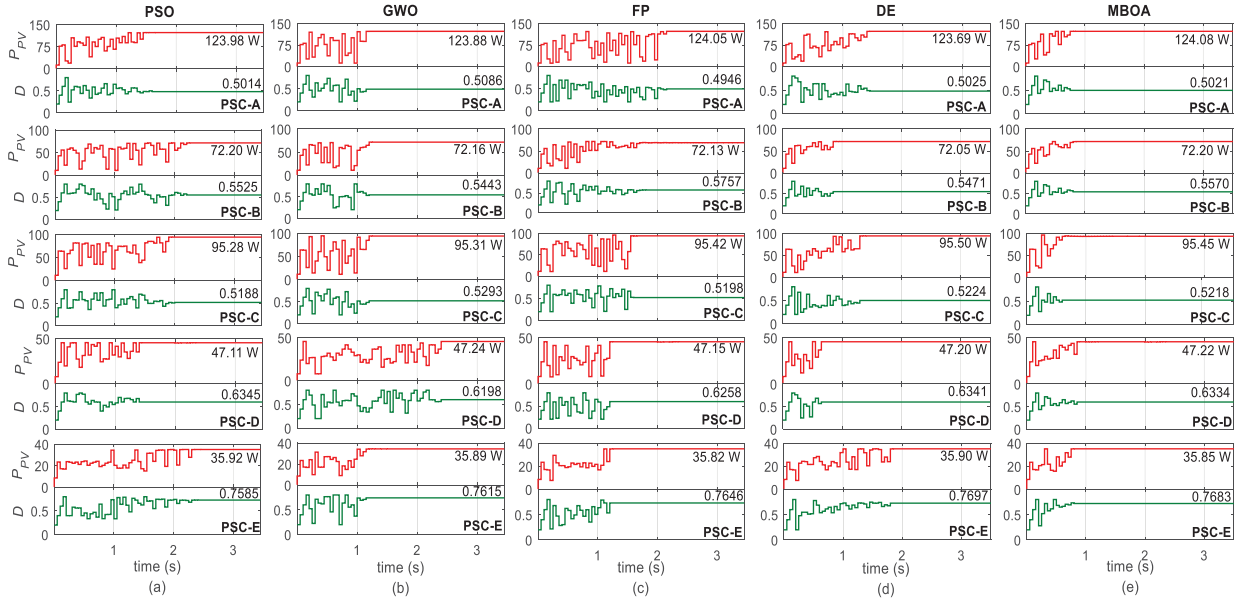

Fig. 12. Comparison for different partial shading patterns between (a) PSO, (b) GWO, (c) FP, (d) DE, and (e) MBOA.

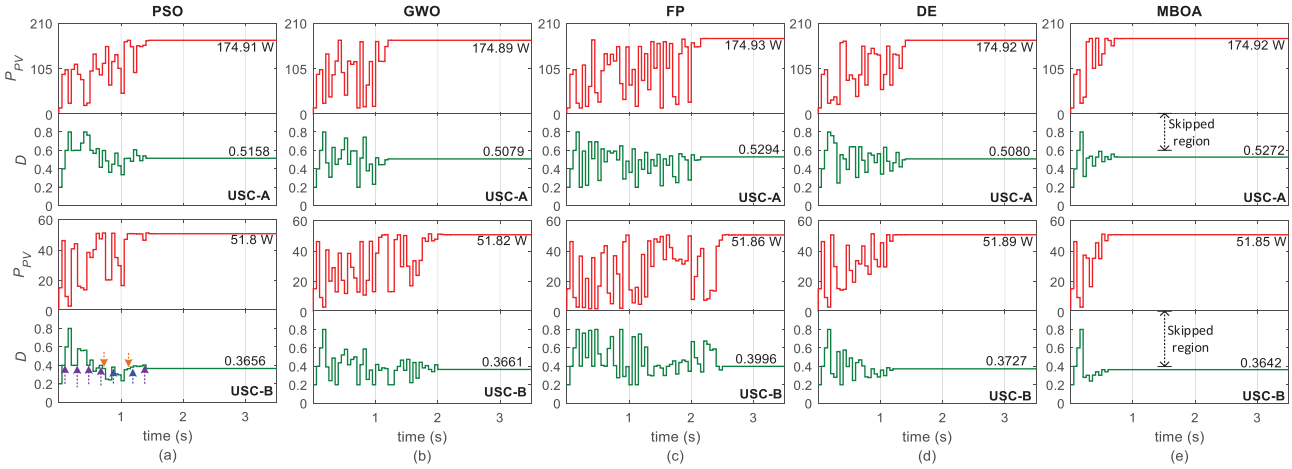

Fig. 13. Comparison for different uniform shading patterns between (a) PSO, (b) GWO, (c) FP, (d) DE, and (e) MBOA.

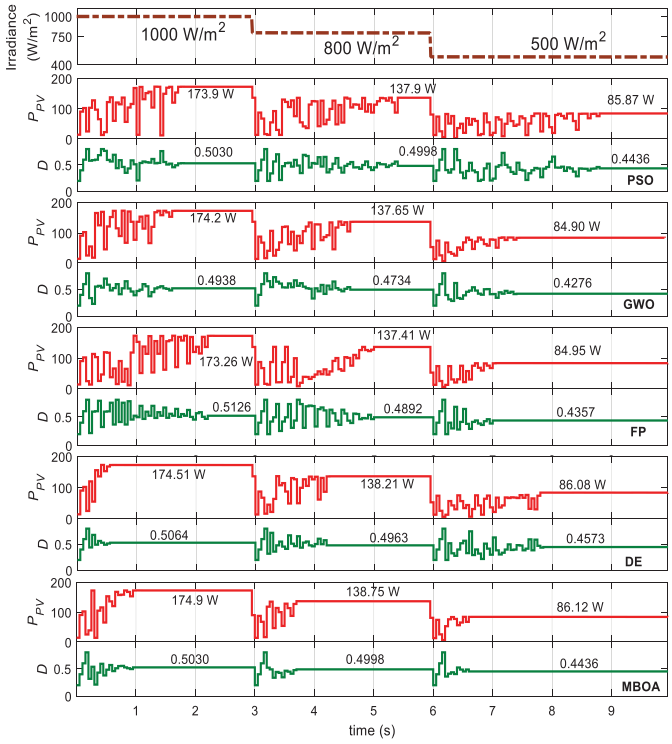

Fig. 14. Response to irradiance transients.

variation is much faster with no high power oscillation. The tracking time for USCs is improved by reducing the search space through skipping method and it can be applied in any conventional isolated or nonisolated dc–dc converter without major modifications required to the proposed controller with the shift in the converter.

VII. Conclusion

In this article, a modified BOA has been proposed for the MPPT tracking, which has the capability to distinguish between partially shaded, uniformly shaded, solar intensity, and load variation conditions. The experimental results proved that different shading patterns were tracked in less than 1 s on average, with 99.85% of steady-state efficiency while avoiding the repetition of the same position in search space. The proposed skipping technique for uniform shaded conditions improved the CS by 47.20%. The response to load variation has been improved by 86.15% while avoiding the reinitialization of the butterflies' position. The most significant advantage of modified BOA in comparison with other MPPT algorithms based on metaheuristic approach is that only one parameter ($t_{\max}$) is required to be chosen depending on V_{oc} of a PV panel making the algorithm implementation much simpler without any cumbersome tuning of parameters by trial and error method. The comparison Table III states that the proposed algorithm consists of higher features in comparison with other metaheuristic algorithms used for MPPT. The future work will focus on the comparative analysis of the MBOA-MPPT implementation on other conventional dc–dc converters practically.

References

[1] T. W. BANK, "Population growth (annual %)," [Online]. Available: https://data.worldbank.org/indicator/SP.POP.GROW

[2] I. Capellán-Pérez, M. Mediavilla, C. de Castro, Ó. Carpintero, and L. Miguel, "Fossil fuel depletion and socio-economic scenarios: An integrated approach," *Energy*, vol. 77, 2014, pp. 641–666, ISSN 0360-5442, https://doi.org/10.1016/j.energy.2014.09.063

[3] K. Aanesan, S. Heck, and D. Pinner, "Solar power. Darkest before dawn," 2017. [Online]. Available: https://www.semanticscholar.org/paper/Solar-power%3A-Darkest-before-dawn-Aanesen-Heck/e42c56b0be121dc5aa89086384fe69757afedcb3

[4] F. B., "Mid-term renewable energy market report," 2015. [Online]. Available: https://www.iea.org/reports/medium-term-renewable-energy-market-report-2015

[5] Z. Q. Wu and D. Q. Yu, "Application of improved bat algorithm for solar PV maximum power point tracking under partially shaded condition," *Appl. Soft Comput.*, vol. 62, pp. 101–109, Jan 2018.

[6] A. Bidram, A. Davoudi, and R. S. Balog, "Control and circuit techniques to mitigate partial shading effects in photovoltaic arrays," *IEEE J. Photovolt.*, vol. 2, no. 4, pp. 532–546, Oct. 2012.

[7] A. Maki and S. Valkealahti, "Power losses in long string and parallel-connected short strings of series-connected silicon-based photovoltaic modules due to partial shading conditions," *IEEE Trans. Energy Convers.*, vol. 27, no. 1, pp. 173–183, Mar. 2012.

[8] H. L. Jou, K. D. Wu, J. C. Wu, C. H. Chung, and D. F. Huang, "Voltage equalizing of solar modules for shadowing compensation," *J. Power Electron.*, vol. 17, pp. 514–521, Mar. 2017.

[9] D. Pilakkat and S. Kanthalakshmi, "An improved P&O algorithm integrated with artificial bee colony for photovoltaic systems under partial shading conditions," *Solar Energy*, vol. 178, pp. 37–47, 2019.

[10] R. Ahmad, A. F. Murtaza, and H. A. Sher, "Power tracking techniques for efficient operation of photovoltaic array in solar applications—A review," *Renewable Sustain. Energy Rev.*, vol. 101, pp. 82–102, Mar. 2019.

[11] N. Kumar, I. Hussain, B. Singh, and B. K. Panigrahi, "Maximum power peak detection of partially shaded PV panel by using intelligent monkey king evolution algorithm," *IEEE Trans. Ind. Appl.*, vol. 53, no. 6, pp. 5734–5743, Nov./Dec. 2017.

[12] M. Seyedmahmoudian, T. K. Soon, B. Horan, A. Ghandhari, S. Mekhilef, and A. Stojcevski, "New ARMO-based MPPT technique to minimize tracking time and fluctuation at output of PV systems under rapidly changing shading conditions," *IEEE Trans. Ind. Inform.*, doi: 10.1109/TII.2019.2895066.

[13] E. Koutroulis and F. Blaabjerg, "A new technique for tracking the global maximum power point of pv arrays operating under partial-shading conditions," *IEEE J. Photovolt.*, vol. 2, no. 2, pp. 184–190, Apr. 2012.

[14] T. L. Nguyen and K. Low, "A global maximum power point tracking scheme employing direct search algorithm for photovoltaic systems," *IEEE Trans. Ind. Electron.*, vol. 57, no. 10, pp. 3456–3467, Oct. 2010.

[15] Y. Ji, D. Jung, J. Kim, J. Kim, T. Lee, and C. Won, "A real maximum power point tracking method for mismatching compensation in PV array under partially shaded conditions," *IEEE Trans. Power Electron.*, vol. 26, no. 4, pp. 1001–1009, Apr. 2011.

[16] R. B. A. Koad, A. F. Zobaa, and A. El-Shahat, "A novel MPPT algorithm based on particle swarm optimization for photovoltaic systems," *IEEE Trans. Sustain. Energy*, vol. 8, no. 2, pp. 468–476, Apr. 2017.

[17] N. Kumar, I. Hussain, B. Singh, and B. K. Panigrahi, "MPPT in dynamic condition of partially shaded PV system by using WODE technique," *IEEE Trans. Sustain. Energy*, vol. 8, no. 3, pp. 1204–1214, Jul. 2017.

[18] K. Sundareswaran, P. Sankar, P. S. R. Nayak, S. P. Simon, and S. Palani, "Enhanced energy output from a PV system under partial shaded conditions through artificial bee colony," *IEEE Trans. Sustain. Energy*, vol. 6, no. 1, pp. 198–209, Jan. 2015.

[19] C. Manickam, G. P. Raman, G. R. Raman, S. I. Ganesan, and N. Chilakapati, "Fireworks enriched P&O algorithm for GMPPT and detection of partial shading in PV systems," *IEEE Trans. Power Electron.*, vol. 32, no. 6, pp. 4432–4443, Jun. 2017.

[20] S. Mohanty, B. Subudhi, and P. K. Ray, "A new MPPT design using grey wolf optimization technique for photovoltaic system under partial shading conditions," *IEEE Trans. Sustain. Energy*, vol. 7, no. 1, pp. 181–188, Jan. 2016.

[21] K. S. Tey, S. Mekhilef, H. T. Yang, and M. K. Chuang, "A differential evolution based MPPT method for photovoltaic modules under partial shading conditions" *Int. J. Photoenergy*, vol. 2014, 2014, Art. no. 945906.

[22] M. Seyedmahmoudian *et al.*, "Simulation and hardware implementation of new maximum power point tracking technique for partially shaded PV system using hybrid DEPSO method," *IEEE Trans. Sustain. Energy*, vol. 6, no. 3, pp. 850–862, Jul. 2015.
[23] T. T. Pei, X. H. Hao, and Q. Gu, "A novel global maximum power point tracking strategy based on modified flower pollination algorithm for photovoltaic systems under non-uniform irradiation and temperature conditions," *Energies*, vol. 11, Oct. 2018, Art. no. 2708.
[24] N. Aouchiche, M. S. Aitcheikh, M. Becherif, and M. A. Ebrahim, "AI-based global MPPT for partial shaded grid connected PV plant via MFO approach," *Solar Energy*, vol. 171, pp. 593–603, Sep. 2018.
[25] K. S. Tey, S. Mekhilef, M. Seyedmahmoudian, B. Horan, A. T. Oo, and A. Stojcevski, "Improved differential evolution-based MPPT algorithm using SEPIC for PV systems under partial shading conditions and load variation," *IEEE Trans. Ind. Inform.*, vol. 14, no. 10, pp. 4322–4333, Oct. 2018.
[26] K. S. Tey and S. Mekhilef, "Modified incremental conductance algorithm for photovoltaic system under partial shading conditions and load variation," *IEEE Trans. Ind. Electron.*, vol. 61, no. 10, pp. 5384–5392, Oct. 2014.
[27] S. Arora and S. Singh, "Butterfly optimization algorithm: A novel approach for global optimization," *Soft Comput.*, vol. 23, pp. 715–734, Feb. 2019.
[28] J. Ahmed and Z. Salam, "An accurate method for MPPT to detect the partial shading occurrence in a PV system," *IEEE Trans. Ind. Inform.*, vol. 13, no. 5, pp. 2151–2161, Oct. 2017.
[29] Y. H. Liu, S. C. Huang, J. W. Huang, and W. C. Liang, "A particle swarm optimization-based maximum power point tracking algorithm for PV systems operating under partially shaded conditions," *IEEE Trans. Energy Convers.*, vol. 27, no. 4, pp. 1027–1035, Dec. 2012.

Immad Shams (Student Member, IEEE) was born in May 1993. He received the M.Eng. degree electrical power from the University of Technology Malaysia, Johor Bahru, Malaysia, in 2017, respectively. He is currently working toward the Ph.D. degree with the Department of Electrical Engineering, University of Malaya, Malaysia.

He has been associated with Power Electronics and Renewable Energy Research Laboratory, as a Graduate Research Assistant, since 2018. His research interests include metaheuristic and bioinspired algorithms, renewable energy, solar based dc–dc power converter topologies and their control, storage devices and energy efficiency.

Mr. Shams was a recipient of the Best Postgraduate Student Award from the University of Technology, Malaysia, Johor Bahru, Malaysia, in 2017.

Saad Mekhilef (Senior Member, IEEE) received the B.Eng. degree in electrical engineering from the University of Setif, Setif, Algeria, in 1995, and the M.Eng. degree in engineering science and the Ph.D. degree in electrical engineering from the University of Malaya, Kuala Lumpur, Malaysia, in 1998 and 2003, respectively.

He is currently a Professor and the Director with the Power Electronics and Renewable Energy Research Laboratory, Department of Electrical Engineering, University of Malaya, where he is also the Dean of the Faculty of Engineering. He is also a Distinguished Adjunct Professor with the Faculty of Science, Engineering and Technology, School of Software and Electrical Engineering, Swinburne University of Technology, VIC, Australia. He has authored or coauthored more than 400 publications in international journals and conference proceedings. His current research interests include power converter topologies, control of power converters, renewable energy, and energy efficiency.

Kok Soon Tey (Member, IEEE) received the B.Eng. degree in electrical engineering and the Ph.D. degree from the University of Malaya, Kuala Lumpur, Malaysia, in 2011 and 2014, respectively.

Since 2011, he has been a Research Assistant with the Power Electronics and Renewable Energy Research Laboratory, Department of Electrical Engineering, University of Malaya, where he was a Senior Lecturer with the Department of Computer System and Information Technology, Faculty of Computer Science and Information Technology in 2015. His research interests include renewable energy control systems, energy management, power efficiency and inverter control of PV systems.